Multirate Adaptive Robust Control with Friction Estimation and Compensation for Tilting Table Machine Tools

Chenyu Ge, Binh-Minh Nguyen, Hiroshi Fujimoto
The University of Tokyo
5-1-5, Kashiwanoha, Kashiwa, Chiba, 277-8561, Japan
ge.chenyu22@edu.k.u-tokyo.ac.jp
nguyen.binhminh@edu.k.u-tokyo.ac.jp, fujimoto@k.u-tokyo.ac.jp

Yuki Terada, Masataka Sakamoto
DMG MORI CO., LTD
2-1, Sanjohonmachi, Nara, Nara, 630-8122, Japan
yk-terada@dmgmori.co.jp
ma-sakamoto@dmgmori.co.jp

***Abstract*—This paper proposes an advanced position control system for the 5-axis machine tool with a tilting table. The challenge is to simultaneously deal with two types of nonlinearity: the position-dependent nonlinearity of unbalanced torque, and the velocity-dependent nonlinearity of Coulomb friction. To overcome this issue, this paper develops a double-layer parameter identification (DLPID) based on the conditional recursive-least square algorithm. The DLPID provides the realtime estimation of not only the inertia, damping, and the maximum unbalance torque but also the friction coefficient. We established a two-degree-of-freedom control configuration in which the multi-rate feedforward controller and the multirate nonlinearity compensator (MNC) are adaptively updated by the DLPID. Experiment results show that the proposed control system can reduce the root-mean-square deviation of the position tracking by up to 62.3% in comparison with a conventional PID controller.**

***Index Terms*—Machine Tools, High-precision Motion Control, Nonlinearity Estimation and Compensation**

I. Introduction

Machine tool plays an irreplaceable role in manufacturing industry. One of the most advanced type of machine tools, as shown in Fig. 1, is the five-axis machine who consists 3 DoFs of translation and 2 DoFs of rotation.

Considering the advanced tool machines, the position accuracy is the most essential requirement. To this end, it is necessary to develop the system with the two-degree-of-freedom (2DoF) configuration includes a feedback controller and a feedforward controller. This study focuses on the feedforward controller, which compensates multiple nonlinear disturbances before they affect the system [2]. The model-based feedforward controllers have been proposed [3]. However, good performance of such controllers were achieved only when we can precisely know the system model, including the nonlinearity. To overcome such problems, adaptive feedforward control with compensation against nonlinearity was proposed [4]. However, this study does not consider the multi-sampling times, which is a real practical issue in the machine tool control. Friction estimation and compensation is introduced in [5], [6] and [7], but within their work, the estimation didn't include other dynamics and without considering modeling uncertainty. Besides, data-driven learning [8] [9] controllers have been developing to reduce the dynamics modeling effort. However, this method requires offline tuning process, which increases the burden to design and implement the controller in practical applications.

Fig. 1. The overview of five-axis machine tool: 3 DoFs of translation(X-Y-Z) and 2 DoFs of rotation(A-C) [1].

With respect to the above discussion, this paper aims to develop a multirate position control system with two degree of freedom configuration. Motivated by the Multirate Adaptive Robust Control (MARC) developed by Fujimoto et al [10], we proposed in [11] an adaptive control system which can online compensates the position dependent nonlinearity. However, [11] does not address the existence of the friction term where in this paper we propose a double-layer parameter identification (DLPID) to simultaneously estimate the inertia and damping along with the friction and unbalanced torque. Furthermore, we propose a multirate nonlinear compensator (MNC) to compensate these nonlinearities. The effectiveness and repeatability of the proposed method has been evaluated by both simulation and experiment using a testbench developed at our research group.

II. System Modeling

A. Dynamics Modeling

To study the motion of the tilting table in Fig. 1, this paper utilizes a 2-inertia motor bench as shown in Fig. 2. The load is assumed to be a uniform semi-circular disc, which generates

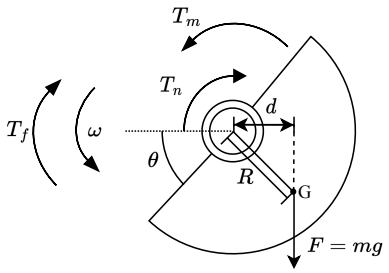

Fig. 2. Model of the testbench in this study.

an extra torque lead by gravity during the rotation of the system and the friction is defined as $T_f = \mathrm{sgn}(\dot{\theta})$.

In the experimental setting of this study, the centre of gravity G is not in the geometric centre. Thus, the torque T_g generated by gravity F is expressed as:

$$T_g = Fd = mgd = FR\mathrm{sin}(\theta) \tag{1}$$

where R is the distance from the centre of gravity to the rotation axis, d is the magnitude of the position, m is the mass of the load and g represents the acceleration of gravity. Here, we define the maximum unbalanced torque $U = FR$. The motion of the testbench is described by the following dynamical equation

$$\underbrace{J\ddot{\theta} + D\dot{\theta}}_{\text{Linear Dynamics}} + \underbrace{U\mathrm{sin}(\theta) + C\mathrm{sgn}(\dot{\theta})}_{\text{Nonlinear Dynamics}} = T_m \tag{2}$$

where the system parameters J is the inertia [$\mathrm{kg\,m^2}$], D is the damping [$\mathrm{N\,m/(rad/s)}$] and C is the coefficient of the friction [$\mathrm{N\,m}$]. Also, we define the total nonlinearity as $T_n = T_g + T_f$.

B. State-space Modeling

For the system described in equation (2), the state space of the model is given below, where the state variable are determined as $\boldsymbol{x} = \begin{bmatrix}\theta & \dot{\theta}\end{bmatrix}^\mathsf{T}$ where θ is the position and $\dot{\theta}$ is the time differentiation of θ and u is the input torque T_m:

$$\begin{aligned}\dot{\boldsymbol{x}} &= \boldsymbol{A}_c\boldsymbol{x} + \boldsymbol{B}_c(u - T_N) = \begin{bmatrix}0 & 1\\ 0 & -\frac{D}{J}\end{bmatrix}\boldsymbol{x} + \begin{bmatrix}0\\ \frac{1}{J}\end{bmatrix}u - \begin{bmatrix}0\\ \frac{1}{J}\end{bmatrix}T_n\\ y &= \boldsymbol{C}_c\boldsymbol{x} = \begin{bmatrix}1 & 0\end{bmatrix}\boldsymbol{x}\end{aligned} \tag{3}$$

The continuous time state-space is discretized to design the feedforward controller in the next section.

III. Control System Design

A. Outline of the Proposal

The proposed control configuration is shown in Fig. 3, including multiple sampling rates, the DLPID, the perfect tracking controller and the PID feedback controller. The discrete variables of $[i]$ are in the sample of reference marked as T_r and those variables of $[k]$ are in the sample of inputs marked as T_y and T_u. In addition, a multirate nonlinear compensator (MNC) is designed to deal with the position dependent nonlinearity and the friction to improve the control performance.

Notice: As presented in [10], by using sensitivity transfer function, it is possible to analyze the robustness or the MARC system against modeling error and disturbance. Global stability with respect to friction nonlinearity can be performed by relay feedback system representation [12] or discontinuous Lyapunov-like function [13]. Due to the limitation of paper space, this paper focuses on the design and implementation of the DLPID instead of the aforementioned analysis.

B. Double-layer Parameter Identification

From (2), the parameters J, D and U can be identified by a RLS algorithm if C is given. On the other hand, if J, D and U are given, the friction coefficient C can be calculated directly. This motivates us to establish a double-layer parameter identification configuration, as shown in Fig. 4.

1) Conditional RLS: RLS is an online parameter estimation tool [10] [14] calculates the system parameters $\boldsymbol{\vartheta} = \begin{bmatrix}J & D & U\end{bmatrix}^\mathsf{T}$, from the input u_{lower} in (4) and the system outputs $\boldsymbol{\varphi} = \begin{bmatrix}\ddot{y} & \dot{y} & \mathrm{sin}y\end{bmatrix}^\mathsf{T}$ using the equation below.

$$u_{lower} = u - u_f = \boldsymbol{\varphi}^T\boldsymbol{\vartheta} = \begin{bmatrix}\ddot{y} & \dot{y} & \mathrm{sin}y\end{bmatrix}\begin{bmatrix}J & D & U\end{bmatrix}^\mathsf{T} \tag{4}$$

The discrete-time RLS algorithm is expressed in (5). Notice that $\boldsymbol{\vartheta}$, $\boldsymbol{L}$ and $\boldsymbol{P}$ are updated only if the persistent excitation (PE) condition stated in (17) is satisfied. Otherwise, $\boldsymbol{\vartheta}[k] = \boldsymbol{\vartheta}[k-1]$, $\boldsymbol{L}[k] = \boldsymbol{L}[k-1]$ and $\boldsymbol{P}[k] = \boldsymbol{P}[k-1]$.

$$\begin{aligned}\hat{\boldsymbol{\vartheta}}[k] &= \hat{\boldsymbol{\vartheta}}[k-1] + \mathrm{Proj}_{\hat{\boldsymbol{\vartheta}}}\{\boldsymbol{L}[k](u_{lower}[k] - \boldsymbol{\varphi}^\mathsf{T}[k]\hat{\boldsymbol{\vartheta}}[k-1])\}\\ \boldsymbol{L}[k] &= \frac{\boldsymbol{P}[k-1]\boldsymbol{\varphi}[k]}{\lambda + \boldsymbol{\varphi}^\mathsf{T}[k]\boldsymbol{P}[k-1]\boldsymbol{\varphi}[k]}\\ \boldsymbol{P}[k] &= \frac{(\boldsymbol{I} - \boldsymbol{L}[k]\boldsymbol{\varphi}^\mathsf{T}[k])\boldsymbol{P}[k-1]}{\lambda}\end{aligned} \tag{5}$$

where $\lambda \in (0, 1]$ is a forgetting factor tuned to obtain good identification performance. The larger λ is, the less it is assumed to be affected by noise and the slower the convergence speed becomes. The projection algorithm bounds the estimated parameters is given as below:

$$\mathrm{Proj}_{\hat{\boldsymbol{\vartheta}}}(\bullet_k) = \begin{cases}0, \text{if } \hat{\boldsymbol{\vartheta}}[k-1] + \bullet_k \geq \boldsymbol{\vartheta}_{max} \text{ and } \bullet_k \geq 0\\ 0, \text{if } \hat{\boldsymbol{\vartheta}}[k-1] + \bullet_k \leq \boldsymbol{\vartheta}_{min} \text{ and } \bullet_k \leq 0\\ \bullet_j, \text{Otherwise.}\end{cases} \tag{6}$$

There are several practical way to verify the PE condition proposed in [14] and [15]. The persistent excitation condition can be verified through calculating the PE matrix $\boldsymbol{M}[k]$ expressed in (7):

$$\boldsymbol{M}[k] = \frac{1}{W}\sum_{l=k-W}^{k}\boldsymbol{\varphi}[l]\boldsymbol{\varphi}^\mathsf{T}[l] \tag{7}$$

In this study, the PE condition is verified by using the moving window with the length $W = 100$. We only need to examine the minimum eigenvalue of matrix $\boldsymbol{M}[k]$, defined as $\kappa[k]$, and PE condition is satisfied when $\kappa[k] > 0$. We will lately show the PE index with desired trajectory in Fig. 6.

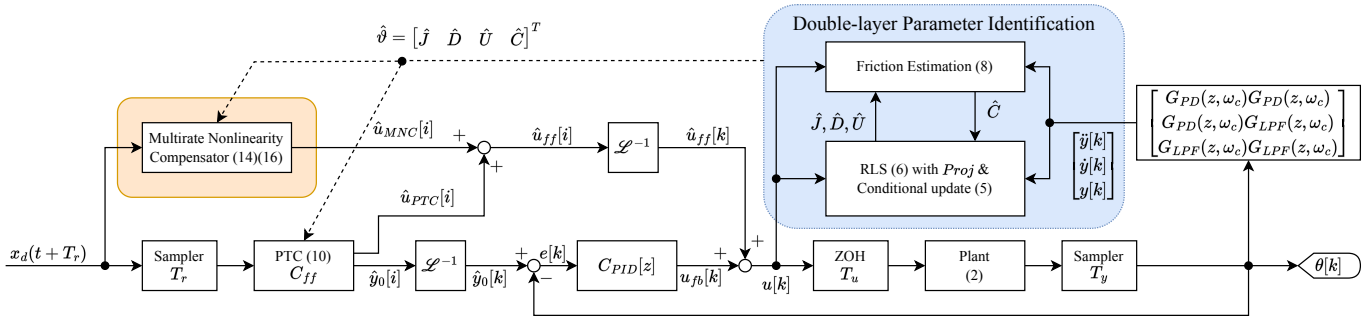

Fig. 3. The proposed configuration of the multirate adaptive robust control system and the main contribution is highlighted. $G_{PD}(z,\omega_c)$ is a discrete pseudo-differentiation and $G_{LPF}(z,\omega_c)$ is a discrete low-pass filter with the cut-off frequency of ω_c.

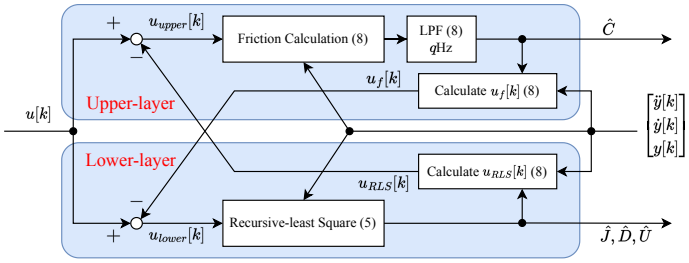

Fig. 4. The schematic of the proposed double-layer parameter identification. The previous research estimated the $\hat{J}$, $\hat{D}$ and $\hat{U}$ only with the lower-layer.

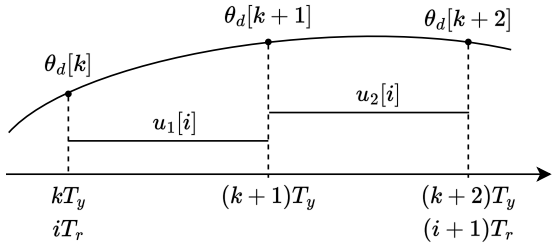

Fig. 5. The schematic of the multirate system [10].

2) The Friction Estimation: The friction coefficient is calculated as follows:

$$\begin{aligned} u_f[k] &= \hat{C}[k-1]\text{sgn}(\dot{y}[k]) \\ u_{RLS}[k] &= \hat{J}[k-1]\ddot{y}[k] + \hat{D}[k-1]\dot{y}[k] + \hat{U}[k-1]\text{sin}(y[k]) \\ \hat{C}[k] &= G_{LPF}[z,q]\frac{u[k]-u_{RLS}[k]}{\text{sgn}(\dot{y}[k])} \end{aligned} \tag{8}$$

where $G_{LPF}[z,q]$ is a discrete low-pass filter with a cut-off frequency of q Hz. The calculated friction $\hat{C}$ is used to compensate the friction online.

C. Adaptive Perfect Tracking Controller

The MARC theory in [10] includes a PID controller and an adaptive PTC which we are going to introduce in this section. There are 2 sampling rates exist within the digital control system to avoid a plant becomes non-minimum phase in discrete-time domain and to reduce computational burden, T_r refers to the sampling rate of the desired trajectory, T_u refers to the sampling rate of the feedforward signal and T_y refers to the sampling rate of the encoder. The illustration of these sampling rates are shown in Fig. 4, for this testbench is a second order system, we select $T_r = 2T_y = 2T_u$ and θ_d denotes the desired trajectory in position.

1) Formulation of PTC: The multirate PTC is designed based on the discretized linear part of (2) following the multirate PTC theory [3] [10].

$$\begin{aligned} \boldsymbol{x}[k+1] &= \boldsymbol{A}_d\boldsymbol{x}[k] + \boldsymbol{B}_d u[k] \\ y[k] &= \boldsymbol{C}_d\boldsymbol{x}[k] \\ \boldsymbol{A}_d = e^{\boldsymbol{A}_c T_y}, \quad \boldsymbol{B}_d &= \int_0^{T_y} e^{\boldsymbol{A}_c\tau}\boldsymbol{B}_c d\tau, \quad \boldsymbol{C}_d = \boldsymbol{C}_c \end{aligned} \tag{9}$$

For the nonadaptive PTC, the multirate plant is given as:

$$\begin{aligned} \boldsymbol{x}_d[i+1] &= \boldsymbol{A}\boldsymbol{x}_d[i] + \boldsymbol{B}\boldsymbol{u}_{PTC}[i] \\ \boldsymbol{y}_0[i] &= \boldsymbol{C}\boldsymbol{x}_d[i] + \boldsymbol{D}\boldsymbol{u}_{PTC}[i] \\ \left[\begin{array}{c|c} \boldsymbol{A} & \boldsymbol{B} \\ \hline \boldsymbol{C} & \boldsymbol{D} \end{array}\right] &= \left[\begin{array}{c|cc} \boldsymbol{A}_d^2 & \boldsymbol{A}_d\boldsymbol{B}_d & \boldsymbol{B}_d \\ \hline \boldsymbol{C}_d & 0 & 0 \\ \boldsymbol{C}_d\boldsymbol{A}_d & \boldsymbol{C}_d\boldsymbol{B}_d & 0 \end{array}\right] \end{aligned} \tag{10}$$

where the state variable $\boldsymbol{x}_d[i]$ is the desired reference $\boldsymbol{x}_d(t)$ sampled by the rate of T_r, the outputs of PTC ($C_f f$) in Fig. 3 are $\hat{u}_{PTC}[i]$ and $\hat{y}_0[i]$ in (10).

The discrete-time lifting operator $\mathscr{L}^{-1}$ in Fig. 3 is to transform the 2-dimension discrete-signal in a rate of T_r to a 2-serial discrete-signal in the rate of T_u.

2) Adaptive PTC: The adaptive PTC will use the estimation of system parameters $\boldsymbol{\vartheta}$ from the RLS, which is $\hat{\boldsymbol{\vartheta}}$, to update the multirate state-space matrices in (10) and mark them as $\hat{\boldsymbol{A}}$, $\hat{\boldsymbol{B}}$, $\hat{\boldsymbol{C}}$, $\hat{\boldsymbol{D}}$. The feedforward command of adaptive PTC is:

$$\hat{\boldsymbol{u}}_{PTC}[i] = \hat{\boldsymbol{B}}^{-1}(\boldsymbol{x}_d[i+1] - \hat{\boldsymbol{A}}\boldsymbol{x}_d[i]) \tag{11}$$

D. Multirate Nonlinearity Compensator

To deal with the nonlinearity, we designed a compensator, in Fig. 3, covering the position-dependent unbalanced torque

TABLE I
SIMULATION SETTING

	J	D	U	C
System Plant	50e-4	130e-4	0.3	0.02
Previous MARC(λ)	20e-4 (0.999)	100e-4 (0.999)	0.1 (0.995)	N/A
Proposed MARC(λ)	20e-4 (0.999)	100e-4 (0.999)	0.1 (0.995)	0.01

and the friction. The output of the MNC is expressed as:

$$\boldsymbol{u}_{MNC}[i] = \boldsymbol{u}_{UBT}[i] + \boldsymbol{u}_f[i] \tag{12}$$

where the u_{UBT} stands for the compensation of the unbalanced torque and u_f stands for the compensation of friction.

1) Unbalanced Torque Compensation: We can calculate the feedforward to compensate the unbalanced torque in (2) from the desired trajectory.

$$\boldsymbol{u}_{UBT}[i] = \begin{bmatrix} U\sin(\theta_d[k]) & U\sin(\theta_d[k+2]) \end{bmatrix}^{\mathsf{T}} \tag{13}$$

For the adaptive case, the U in (13) can be replaced by $\hat{U}$ from the RLS identification.

2) Friction Compensation: The model used to compensate the total friction [5] is given as:

$$T_f(\omega_d) = \frac{\hat{C}}{\pi}(\tan^{-1}(\alpha(\omega_d - \omega_{th}))) + \tan^{-1}(\alpha(\omega_d + \omega_{th})) \tag{14}$$

where T_f is the feedforward torque to compensate friction, $\hat{C}$ is the estimated friction, α is a constant which in the case $\alpha = 1 \times 10^4$ and $\omega_{th} = 0.05$ marks a dead zone. The feedforward signal to compensate the friction is designed as:

$$\boldsymbol{u}_f[i] = \begin{bmatrix} T_f(\dot{\theta}[k]) & T_f(\dot{\theta}[k+2]) \end{bmatrix}^{\mathsf{T}} \tag{15}$$

To cooperate with the PTC, the nonlinearity feedforward is designed with a sapling rate of T_r.

IV. SIMULATION VALIDATION

A. Simulation Setup

In this paper, a practical approach is utilized to select the aforementioned gains of the control system. The PID controller gains are calculated by pole-placement to the close-loop system including the PID and the nominal plant $G_n(s) = (J_n s^2 + D_n s)^{-1}$ in -10π, where J_n and D_n are the same as the initial estimations in Table I. Using Matlab/Simulink and the parameter in Table I, we established a simulator which imitates the real system. The initial estimations of RLS are the same as the nominal plants. For a measurement noise within $\pm 1 \times 10^{-5}$ rad is introduced in the simulator, the LPF of the parameter identifications can be selected with relative lower value of the cut-off frequency. For a clear demonstration of the fine tuning, in the following simulation, we will examine the LPF with the cut-off frequency of 100 Hz and 2 Hz, respectively.

The reference trajectory and the PE index are shown in Fig. 6 and the PE conditions in this research are shown as:

$$\theta > 0.1 \text{ rad or } |\dot{\theta}| > 0.2 \text{ rad/s or } |\ddot{\theta}| > 0.5 \text{ rad/s}^2 \tag{16}$$

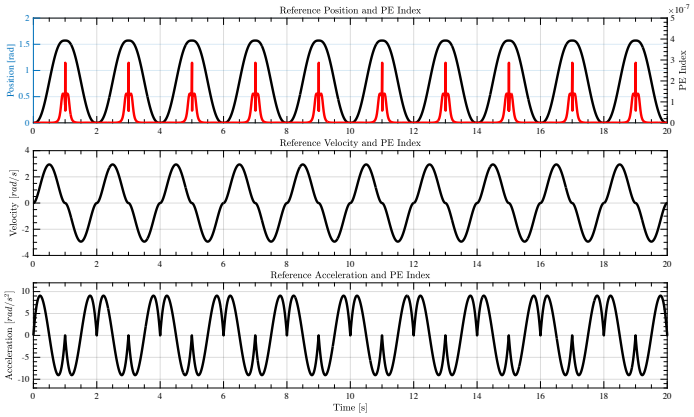

Fig. 6. The desired trajectory with pre-calculated PE index ($\kappa > 0$) used in simulations and experiments.

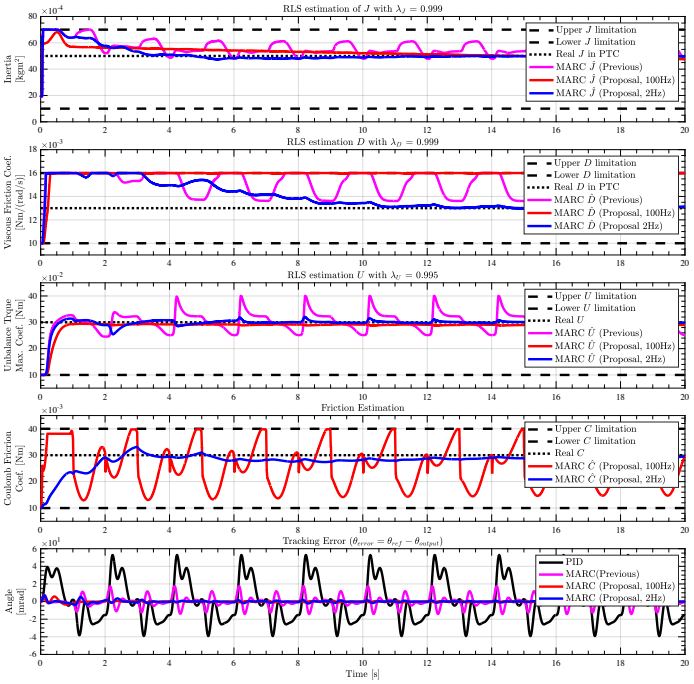

Fig. 7. The simulation result of PID, previous MARC and the proposed MARC with different setting of low-pass filter.

Specifically saying, U is updated when $\theta > 0.1$, D is updated when $|\dot{\theta}| > 0.2$ and J is updated when $|\ddot{\theta}| > 0.5$.

For a fair comparison, we compared our proposal with PID feedback and our previous research in [11]. Our previous research, comparing with this research, was a single layer estimation lacking of the friction estimation and compensation. We applied RLS algorithm to estimate the J, D and U, despite of the friction term C in our simulation plant and testbench. The compensation, shown in (18), included the position-dependent unbalanced torque only.

$$\boldsymbol{u}_{MNC0}[i] = \begin{bmatrix} U\sin(\theta_d[k]) & U\sin(\theta_d[k+2]) \end{bmatrix}^{\mathsf{T}} \tag{17}$$

Such strategy caused a periodical vibration on the estimation

of J, D and U for the reason that the friction changed periodically and influenced the estimation, we can confirm it from the results of simulations and experiments. The simulation setting of J, D and U for the previous MARC is shown in Table I.

B. Simulation Results

In Fig. 7, the tracking performance is improved significantly using the proposed MARC combined with MNC to compensate both position-dependent nonlinearity and friction. The proposed MARC with a LPF, cut-off frequency of 2Hz, the tracking performance increased up to 96.2% evaluated using RMSD of error. Notice that the estimation and tracking error influenced by the friction is reduced significantly thanks to the friction compensation.

V. Experimental Validation

A. Experimental Setup

The experimental system is shown in Fig. 8. The unbalanced load(s) simulates the tilting table and they are connected by a damping. The loads are powered by 2 motors with same input current command. The motor has the rated power of 1.6 kW, the rated torque of 5.09 Nm, and the peak torque of 15.27 Nm. The control system is implemented in C program and the fundamental sampling rate $T_u = T_y = 4 \times 10^{-4}$ s, the sampling rate of the reference signal $T_r = 8 \times 10^{-4}$ s and in concern of the computational burden and anti-noise the RLS algorithm can be performed with a longer period $T_{RLS} = 4 \times 10^{-3}$ s. In the experiment, the sensor measurements suffer from noises which would cause fluctuation in the identified parameters. Through a fine-tuning process, we selected the cut-off frequency of 1 Hz, which coincides with the period when the velocity crosses the 0 point.

There are 2 series of experiments: a) Comparison between the PID, the previous MARC algorithm and the proposed MARC in this research. b) Validation of the repeatability of the proposed MARC algorithm.

B. Experiment Results

The experiment results are shown in Fig. 10, where the green dash lines marks the limitation of the estimation respectively for J, D, U, C and the experiment results are different from the simulations for the reason that we didn't identify these parameters offline.

The proposed method compensated the friction and transparently reduced the position tracking error. The tracking performance of the proposed method is, 62.3% in maximum, better than the conventional PID controller and the previous MARC which only considered the unbalanced torque.

The RMSD of the error in those 4 simulations along with 2 series of experiments is given in Fig. 9. The percentages marks the RMSD compare within each series respectively. Because of the complexity of the experimental environment, the control performances in experiments are relatively different from the simulation case. Despite of that, the proposed method in this case still shows a better performance, a more stable estimation and a more accurate tacking, compare with the PID controller and the MARC algorithm in the previous research.

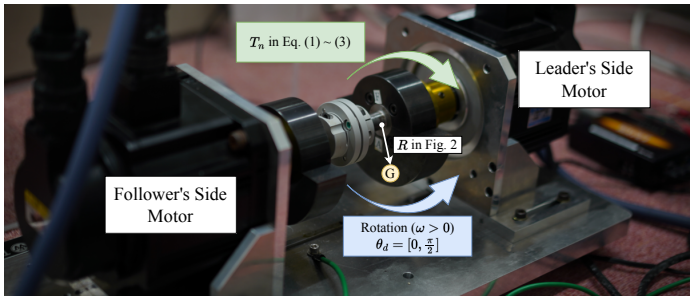

Fig. 8. Unbalance torque testbench used in this study.

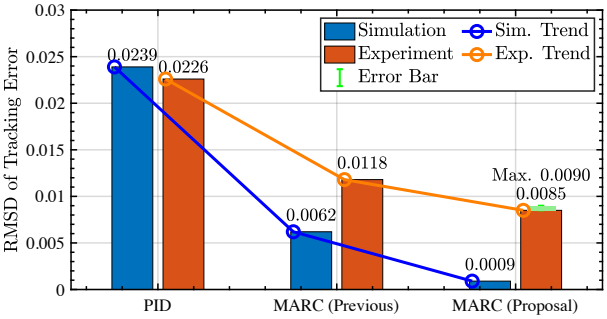

Fig. 9. RMSD of tracking error [rad] in simulations and experiments.

VI. Conclusions and Outlooks

In this study, we presented a multirate approach towards nonlinear estimation and compensation based on the RLS algorithm. We show that it is possible to estimate both nonlinearities under initial modeling uncertainty. The effectiveness of the proposal has been verified by both numerical simulations and experiments. Simultaneous compensation shows remarkably contribution to improve the tracking performance in comparison with the control system consisting only the PID controller. In future, we will attempt to explore more stable and efficient ways to estimate the friction. Also, we will improve the MNC algorithm to achieve a better intersample performance. Besides, we will investigate the design approach that rigorously guarantee the stability of the system with respect to the nonlinearity.

Theoretically speaking, it is non-trivial to analyze and guarantee the stability of the overall control system in Fig. 3. An idea is to equivalently represent the system as the feedback connection of two subsystems. The former is the nonlinear dynamics part of the testbench dynamics (2). The later includes the linear part of the testbench dynamics, the controller, and the parameter identification. With respect to the upper-bound and lower-bound of the nonlinear dynamics, there exists several schemes to analyze this feedback connection, such as the Popov criterion [16]. The controller gains, the forgetting factors and the cut-off frequencies of the LPFs in the parameter identification should be carefully selected to satisfy the stablity of the system and the desirable control performance.

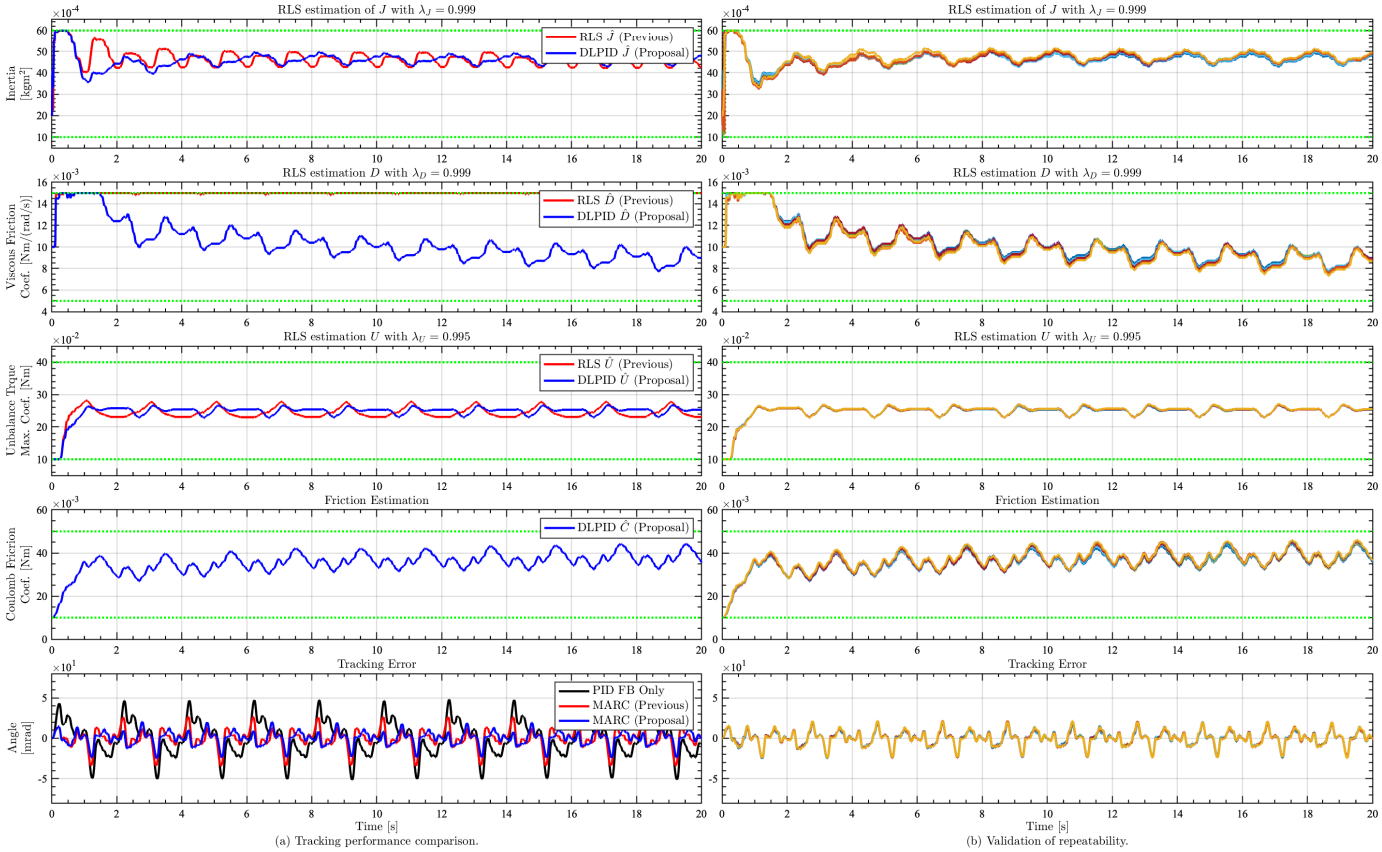

(a) Tracking performance comparison. (b) Validation of repeatability.

Fig. 10. The results of 2 series experiments.

REFERENCES

[1] DMG MORI CO.,LTD, "An Introduction to 5-axis Processing," https://www.dmgmori.co.jp/sp/5axis/ (Accessed on 24th of July, 2023).

[2] L. Blanken, F. Boeren, D. Bruijnen and T. Oomen, "Batch-to-Batch Rational Feedforward Control: From Iterative Learning to Identification Approaches, With Application to a Wafer Stage," IEEE/ASME Transactions on Mechatronics, vol. 22, no. 2, pp. 826-837 (2017).

[3] H. Fujimoto, Y. Hori and A. Kawamura, "Perfect tracking control based on multirate feedforward control with generalized sampling periods," IEEE Transactions on Industrial Electronics, Vol. 48, No. 3, pp. 636-644 (2001).

[4] S.Yabui and I. Tsuyoshi, "Development of Adaptive Feed-Forward Cancellation With Frequency Estimation Algorithm for Compensation of Periodic Disturbance at Arbitrary Frequency," Journal of Dynamic Systems, Measurement, and Control, Vol. 141, No. 12, pp. 121014 (2019).

[5] D. Papageorgiou, M. Blanke, H. Henrik Niemann and J.H. Richter, "Online friction parameter estimation for machine tools" in Advanced Control for Application, Vol. 2, Issue 1, (2020).

[6] S. Katsura, J. Suzuki and K. Ohnishi, "Pushing Operation by Flexible Manipulator Taking Environmental Information Into Account," IEEE Transactions on Industrial Electronics, Vol. 53, No. 5, pp. 1688-1697 (2006).

[7] P. Juan, O, Kiyoshi, Y. Yuki and M. Toshimasa, "Velocity Driven N-order Stick Compensator and Slip Suppressor for Nonlinear Friction in an Oil-Seal-Mounted Geared Motor," IEEJ Journal of Industry Applications, 2020, Vol. 9, No. 2, pp. 168-176 (2020).

[8] W. Ohnishi, S. Nard and O. Tom, "State-tracking Iterative Learning Control in Frequency Domain Design for Improved Intersample Behavior," International Journal of Robust and Nonlinear Control, Vol. 33, No. 7, pp. 4009-4027 (2023).

[9] Y. Inagaki, M. Mae, O. Shimizu, S. Nagai, H. Fujimoto, T. Miyajima, Y. Yasuda and A. Yamagiwa, "Effect of Harmonic Current Suppression on Iron Loss of IPMSM Using Repetitive Perfect Tracking Control," IEEJ Journal of Industry Applications, Vol. 11, No. 2, pp. 317-326 (2022).

[10] H. Fujimoto and B. Yao, "Multirate adaptive robust control for discrete time non-minimum phase systems and application to linear motors," IEEE/ASME Transactions on Mechatronics, Vol. 10, No. 4, pp. 371-377 (2005).

[11] C. Ge, B-M. Nguyen, H. Fujimoto, Y. Terada and M. Sakamoto, "Multirate Adaptive Robust Control with Position-dependent Nonlinearity for Tilting-table of Machine Tool: A Basic Study on Test-bench", IEEJ Technical Meeting on Mechatronics Control, Tokyo, Japan (2023).

[12] S. Jeon and M. Tomizuka, "Stability of A Class of Relay Feedback Systems Arising in Controlled Mechanical Systems with Ideal Coulomb Friction, IFAC paper online, (2008).

[13] A. Bisoffi, M. Da Lio, A. R. Teel and L. Zaccarian, "Global Asymptotic Stability of a PID Control System With Coulomb Friction," in IEEE Transactions on Automatic Control, vol. 63, no. 8, pp. 2654-2661, (2018).

[14] B. Yao and P. Andrew, "Indirect adaptive robust control of SISO nonlinear systems in semi-strict feedback forms," IFAC Proceedings Volumes, Vol. 35, Vo. 1, pp. 397-402, (2001).

[15] K. Ohno, H. Fujimoto, Y. Isaoka and Y. Terada, "Adaptive Cutting Force Observer for Machine Tool Considering Stage Parameter Variation," 2021 IEEE International Conference on Mechatronics (ICM), Kashiwa, Japan, pp. 1-6, (2021).

[16] J. B. Moore, and B. D. O. Anderson, "A generalization of the Popov criterion," Journal of the franklin Institute, Vol. 285, No. 6, pp. 488-492, (1968).